Identification of cadmium vacancy complexes in CdTe(In), CdTe(Cl) and CdTe(I) by positron annihilation with core electrons

1997 J. Phys.: Condens. Matter 9 5495

(http://iopscience.iop.org/0953-8984/9/25/017)

J. Phys.: Condens. Matter **9** (1997) 5495–5505. Printed in the UK PII: S0953-8984(97)81412-9

Identification of cadmium vacancy complexes in CdTe(In), CdTe(Cl) and CdTe(I) by positron annihilation with core electrons

H Kauppinen†, L Baroux‡, K Saarinen†, C Corbel‡ and P Hautojärvi†

† Laboratory of Physics, Helsinki University of Technology, 02150 Espoo, Finland
‡ Institut National des Sciences et Techniques Nucléaires, Centre d'Etudes Nucléaires de Saclay, 91191 Gif-sur-Yvette Cedex, France

Received 29 January 1997, in final form 25 April 1997

Abstract. Doppler-broadening of the 511 keV positron annihilation line was used for defect identification in CdTe materials. In electrically compensated lightly n-type CdTe(In) and lightly p-type or semi-insulating CdTe(Cl) crystals positron lifetime measurements show vacancy defects with characteristic positron lifetimes of 323 ps and 370 ps, respectively. The shapes of the high-momentum parts of the measured electron-momentum distributions indicate that both defects contain a cadmium vacancy V_{Cd}. The defects are assigned to vacancy-donor complexes V_{Cd}-In and V_{Cd}-Cl, respectively. A vacancy in MBE-grown CdTe(I) layers observed with a low-energy positron beam is also identified as a cadmium vacancy V_{Cd} which is most likely complexed with I-donors.

1. Introduction

Recently it has been demonstrated that the Doppler broadening of the 511 keV positron annihilation line can be used for identifying the microscopic structure of vacancy defects in semiconductors [1–7]. The well established positron lifetime technique probes the average electron density in the material, and therefore it measures the open volume and the concentration of vacancy defects [8, 9]. The utility of the Doppler broadening is based on the fact that the high-energy tail of the annihilation line is the momentum distribution of annihilating core electrons. In a localized positron state at a vacancy, this core-electron momentum distribution is a fingerprint of the chemical identity of the neighbour atoms of the vacancy. In our earlier work a theory of the technique was established and the method was applied to several bulk materials and lattice defects, particularly in compound semiconductors [1, 2]. It was shown that in InP the sublattices of the indium and phosphorus vacancies can be experimentally distinguished by the magnitude differences in the core-electron momentum distributions at the vacancies. Moreover, it was demonstrated that a zinc impurity around a vacancy causes a strong broadening in the shape of the measured core-electron momentum distribution and correspondingly a vacancy-zinc complex can be identified. Based on the experimental and theoretical framework, it becomes evident that in several other compounds the sublattice of vacancy defects could also be determined on the basis of the shape of the core-electron momentum distribution. When the electron orbitals of sublattice atoms in a compound are different enough, the high-momentum part of the annihilation line at a vacancy in one sublattice should be broader than that in the

0953-8984/97/255495+11$19.50

other sublattice. In this work we shall show that this is the case in cadmium telluride (Z(Cd) = 48, Z(Te) = 52) and that the positron trap can be identified as a cadmium vacancy.

Point defects play an important role in the electrical properties of CdTe. The technological applications of CdTe (nuclear detectors, epitaxy substrates and electro-optical devices) require material of high resistivity, 10^8–10^9 Ω cm. The high resistivity can be obtained by doping with group II or group VII impurity atoms. The electrical compensation of doped CdTe is due to native point defects. The well known vacancy defects in CdTe are the isolated cadmium vacancy V_{Cd}, the complex V_{Cd}-D of a cadmium vacancy and a donor atom D, the complex V_{Cd}-2D of a cadmium vacancy and two donor atoms and the isolated tellurium vacancy V_{Te}. In semi-insulating CdTe the charge states of these defects are believed to be V_{Cd}^{2-}, $(V_{Cd}\text{-D})^-$, $(V_{Cd}\text{-2D})^0$ and V_{Te}^0, respectively [11–14].

Positron lifetime measurements have confirmed the existence of vacancy defects in impurity-doped electrically compensated CdTe. In In-doped CdTe a vacancy defect with a positron lifetime of 320–330 ps has been observed and in Cl-doped CdTe a vacancy defect with a positron lifetime of 350–380 ps has been detected [16–19]. Since the concentration of these vacancies is seen to increase in conjunction with the donor-impurity concentration, they are assigned to complexes of the cadmium vacancy and the donor atoms.

Low-energy positron beams are widely used for defect studies in thin (∼1 μm) semiconducting overlayers. The core-electron annihilation technique was recently applied to determine the structures of the DX-centres in AlGaAs and AlGaInP layers, as well as to identify Zn and Se vacancies in ZnSSe layers [3–5]. In this work we apply the information gained in CdTe(In) and CdTe(Cl) crystals to defect identification in I-doped n-type CdTe-layers grown by molecular beam epitaxy (MBE). It is shown that in MBE-grown CdTe(I) a cadmium vacancy defect is also observed.

2. Experimental details

The electron momentum distributions can be measured as the Doppler broadening of the annihilation line at 511 keV. Due to the momentum conservation in the annihilation event, the energy of each annihilation photon is shifted from 511 keV by a small amount of energy

$$\Delta E = p_z/2c \tag{1}$$

where p_z is the momentum of the annihilating electron–positron pair projected to the line of emission of the photon. The experimentally detected distribution $P(p_z)$ is the momentum density of the annihilating electrons, because the positron momentum is practically zero.

In this study we are interested in determining the distribution $P(p_z)$ at vacancies in CdTe. As the positron trapping to vacancies is only partial in our samples, the measured distribution $P(p_z)$ is a superposition of the bulk lattice (subscript b) and vacancy (subscript v) responses

$$P(p_z) = (1 - \eta_v)P_b(p_z) + \eta_v P_v(p_z) \tag{2}$$

where η_v is the fraction of positrons annihilating at vacancies. It is therefore necessary to determine η_v by positron lifetime measurements. The experimental positron lifetime spectra are analysed with two exponential components. The average positron lifetime τ_{ave} is calculated from the fitted lifetimes and their intensities as $\tau_{ave} = I_1\tau_1 + I_2\tau_2$. When there is only one vacancy defect acting as a positron trap we have $\tau_1 = (\tau_b^{-1} + \kappa)^{-1}$ and $\tau_2 = \tau_v$, where τ_b is the positron lifetime in the bulk lattice, κ is the positron trapping rate to the

Table 1. In- and Cl-doped CdTe samples: the dopant concentration, the free-carrier concentration at 300 K and the results of the positron lifetime and Doppler-broadening measurements at 300 K. The shape parameters W and S of the annihilation line are calculated by using the momentum windows (12–17) $\times 10^{-3} m_0 c$ and (0–2.4) $\times 10^{-3} m_0 c$, respectively. The presented W and S are normalized to the corresponding values $W = 0.0174(1)$ and $S = 0.4635(6)$, respectively, measured in sample 1.

Sample	Dopant concentration (cm^{-3})	Carrier concentration (cm^{-3})	τ_{ave} (ps)	τ_2 (ps)	W	S
1	Undoped	$p = 5 \times 10^{15}$	287	—	1	1
2	[In] $= 5 \times 10^{15}$	$n = 1 \times 10^{12}$	292	323(3)	0.94(2)	1.000(2)
3	[In] $= 8 \times 10^{16}$	$n = 2 \times 10^{13}$	302	323(3)	0.86(2)	1.005(3)
4	[In] $= 5 \times 10^{17}$	$n = 1 \times 10^{13}$	319	323(3)	0.77(2)	1.014(2)
5	[Cl] $< 1 \times 10^{15}$	$p = 2 \times 10^{12}$	291	370(5)	0.96(2)	0.999(3)
6	[Cl] $= 1 \times 10^{17}$	—	303	370(5)	0.92(2)	1.001(2)
7	[Cl] $= 1 \times 10^{18}$	$p = 5 \times 10^{7}$	312	370(5)	0.89(2)	1.004(3)

vacancy and τ_v is the positron lifetime at the vacancy. The average positron lifetime τ_{ave} is also a superposition of the bulk lattice and vacancy responses [8]:

$$\tau_{ave} = (1 - \eta_v)\tau_b + \eta_v \tau_v. \tag{3}$$

As the decomposition of the positron lifetime spectrum yields τ_{ave} and τ_v, we can solve η_v from equation (3). Then, provided that the bulk distribution $P_b(p_z)$ is known, the distribution $P_v(p_z)$ at the vacancy can be solved from equation (2).

We studied the core-electron momentum distributions in three In-doped and three Cl-doped CdTe crystals, as indicated in table 1. Samples 3–7 are grown with the travelling heater method (THM) and sample 2 is grown with the Bridgman method. The In- and Cl-doped crystals have very low free-carrier concentrations, whereas the dopant concentrations vary in the ranges [In] $= 5 \times 10^{15}$–5×10^{17} cm^{-3} and [Cl] $\leqslant 1 \times 10^{15}$–$1 \times 10^{18}$. An undoped p-type THM-grown CdTe crystal was measured as a reference sample.

Samples 1–7 were measured with a ^{22}Na positron source that was prepared by evaporating ^{22}NaCl on a thin Al-foil. In the Doppler-broadening and positron lifetime measurements the source activities were 18 and 70 μCi, respectively. The source was sandwiched between two identical sample pieces. All measurements were carried out at 300 K.

The Doppler-broadening spectra were measured with the coincidence arrangement that has been described previously [1, 2, 10]. The γ-energy spectrum was recorded with a high-purity (HP) Ge detector and a digitally stabilized multichannel analyser (MCA) system. In order to reduce the background in the high-energy tail of the 511 keV annihilation peak, a NaI scintillation detector was placed in a collinear geometry with the HP Ge detector. The distance from the sample to the detectors was 30 cm. The annihilation event was accepted in the MCA if both annihilation photons were detected in coincidence in the HP Ge and NaI detectors. The peak-to-background ratio on the high-energy side of the annihilation line was 3×10^4 and the count rate was 110 s^{-1}. We registered 1×10^7 annihilation events in each spectrum. The experimental arrangement enables us to compare the momentum distributions $P_b(p_z)$ and $P_v(p_z)$ up to $p_z = 30 \times 10^{-3} m_0 c$. The pile-up in the tail of the annihilation peak was minimized by gating the MCA with a pile-up rejection signal of the spectroscopy amplifier and by using a short shaping time 2 μs in the amplifier. The energy resolution at 511 keV was 1.6 keV ($6.3 \times 10^{-3} m_0 c$). The remaining pile-up was

Table 2. I-doped CdTe samples: the dopant concentration, the free-carrier concentration at 300 K and the results of the Doppler-broadening measurements with a low-energy positron beam at 300 K. The shape parameters S and W of the annihilation line are calculated by using the momentum windows (0–2.4) $\times 10^{-3} m_0 c$ and (12–17) $\times 10^{-3} m_0 c$, respectively. The presented S and W are normalized to the corresponding values $S = 0.5618(2)$ and $W = 0.0174(1)$, respectively, measured in sample 8. S is determined from conventional Doppler-broadening measurements without the coincidence set-up. W is measured with the coincidence system.

Sample	Dopant concentration (cm^{-3})	Carrier concentration (cm^{-3})	S (no coincidence)	W
8	Undoped	—	1	1
9	$[I] = 1 \times 10^{18}$	$n = 1 \times 10^{18}$	1.002(1)	—
10	$[I] = 5 \times 10^{18}$	—	1.015(1)	—
11	$[I] = 2 \times 10^{19}$	$n = 5 \times 10^{18}$	1.018(1)	0.78(1)
12	$[I] = 1 \times 10^{20}$	—	1.019(1)	—
13	$[I] = 3 \times 10^{20}$	$n = 1 \times 10^{18}$	1.018(1)	—

determined by fitting an exponential function to the slowly descending pile-up tail of the spectrum. Its magnitude was only 2% of the area of the spectrum in the momentum range $p_z = (10–30) \times 10^{-3} m_0 c$ and in the final analysis it was subtracted from the spectrum.

The positron lifetimes were measured with a fast–fast coincidence spectrometer with a time resolution of 220 ps. We collected 2×10^6 annihilation events in each spectrum. After source corrections the spectra were analysed with one or two exponential components.

The low-energy positron beam measurements were performed at 300 K for six I-doped CdTe layers grown by molecular beam epitaxy in University of Würzburg (table 2). The 1 μm thick layers had been grown on an undoped CdTe substrate. An undoped MBE-grown CdTe layer was measured as a reference sample. All samples were measured with a conventional Doppler-broadening system without a coincidence set-up. The mean positron penetration depth was scanned from 2.2 nm to 1.2 μm by changing the incident positron energy from 0.5 to 25 keV. We registered 3×10^6 annihilation events in each spectrum.

Samples 8 and 11 were investigated with a coincidence system. The incident positron energy was 9 keV, corresponding to a mean penetration depth of 230 nm in CdTe. With this incident energy, the positrons annihilate in the I-doped layer in sample 11. The γ-detector arrangement was similar to that described above. The peak-to-background ratio was 2×10^4, the coincidence count rate was 60 s^{-1}, and the resolution at 511 keV was 1.2 keV ($4.7 \times 10^{-3} m_0 c$). We collected 2×10^7 annihilation events in each spectrum.

The shape parameters S and W are useful tools for characterizing the momentum distributions $P(p_z)$, $P_b(p_z)$ and $P_v(p_z)$. They are defined as ratios $S = N_S/N_{TOT}$ and $W = N_W/N_{TOT}$, respectively. The integral N_S is the area of a low-momentum region (0–2.4) $\times 10^{-3} m_0 c$ of the distribution, N_W is the area of a high-momentum region (12–17) $\times 10^{-3} m_0 c$ and N_{TOT} is the total area of the distribution.

3. Vacancy defects in CdTe(In) and CdTe(Cl) crystals

3.1. Positron trapping to vacancies

In undoped CdTe only one positron lifetime component of 287 ps is found. As shown in table 1, the average positron lifetime τ_{ave} is higher in CdTe(In) and CdTe(Cl), and it increases

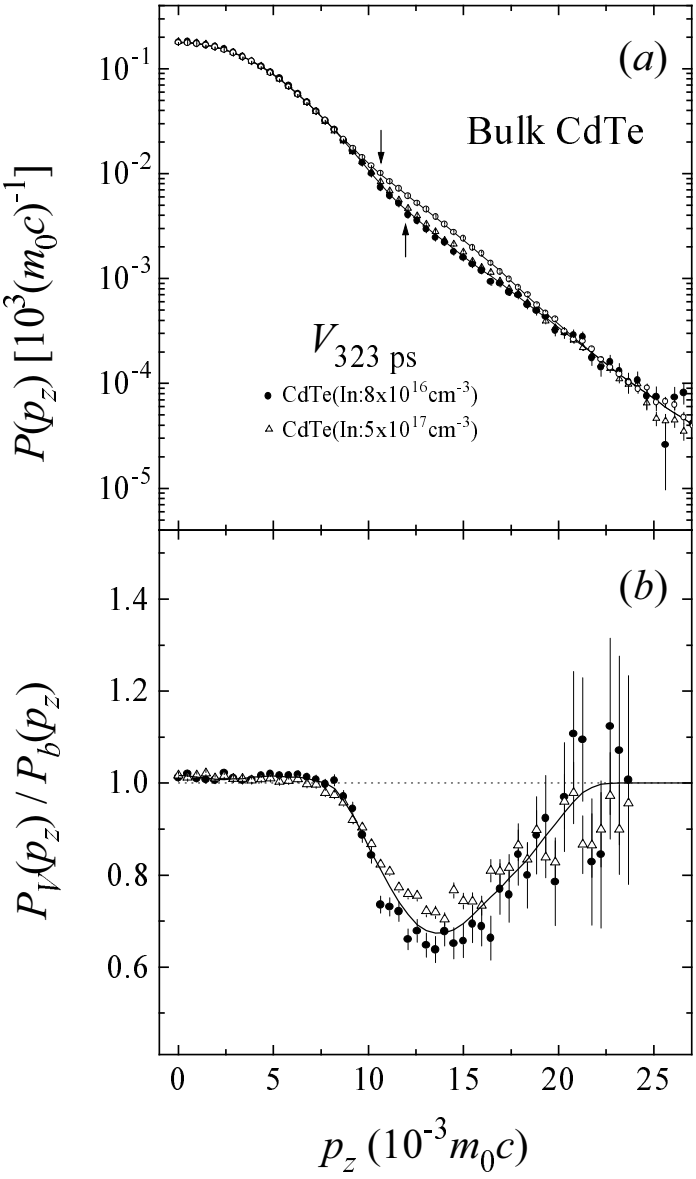

Figure 1. (*a*) Positron annihilation momentum densities $P(p_z)$ at the vacancy corresponding to a positron lifetime 323 ps in CdTe(In) (samples 3 and 4) and in bulk CdTe (sample 1); (*b*) the ratio of the momentum density $P_v(p_z)$ at the 323 ps vacancy (samples 3 and 4) to the momentum density $P_b(p_z)$ in bulk CdTe (sample 1). The full curves are guides to the eye.

with increasing dopant concentration. In CdTe(In) we obtain a second lifetime component $\tau_2 = 323(3)$ ps and in CdTe(Cl) the second lifetime component is $\tau_2 = 370(5)$ ps.

The positron lifetime 287 ps in the undoped sample 1 is characteristic to the free annihilation state in bulk CdTe [15, 16]. The momentum distribution measured in sample 1 thus represents the positron annihilation momentum density $P_b(p_z)$ in the CdTe lattice. In the doped samples the result $\tau_{ave} > \tau_b$ indicates that positrons are trapped to vacancy

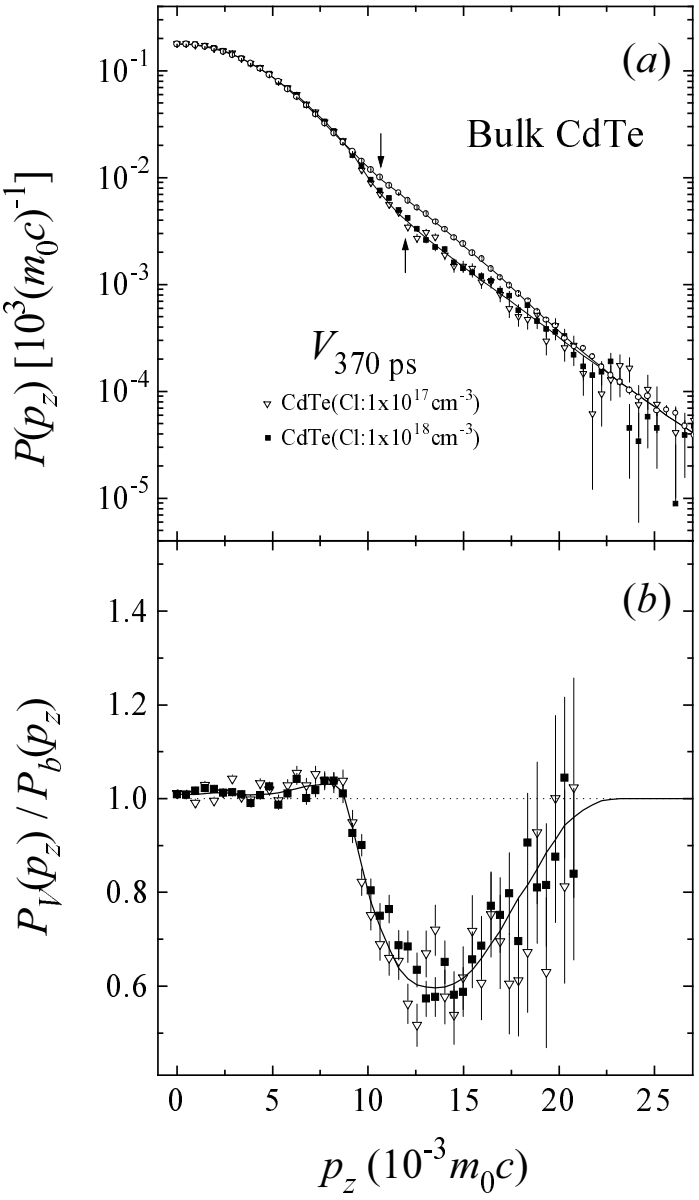

Figure 2. (*a*) Positron annihilation momentum densities $P(p_z)$ at the vacancy corresponding to a positron lifetime 370 ps in CdTe(Cl) (samples 6 and 7) and in bulk CdTe (sample 1); (*b*) the ratio of the momentum density $P_v(p_z)$ at the 370 ps vacancy (samples 6 and 7) to the momentum density $P_b(p_z)$ in bulk CdTe (sample 1). The full curves are guides to the eye.

defects. The characteristic positron lifetimes at the vacancies are $\tau_v = 323$ ps in CdTe(In) and $\tau_v = 370$ ps in CdTe(Cl).

The positron annihilation momentum densities $P_v(p_z)$ at the $V_{323\,ps}$ and $V_{370\,ps}$ vacancies are shown in figures 1 and 2, respectively, together with $P_b(p_z)$. We observe the following. First, the same vacancy response $P_v(p_z)$ is decomposed in samples where the positron

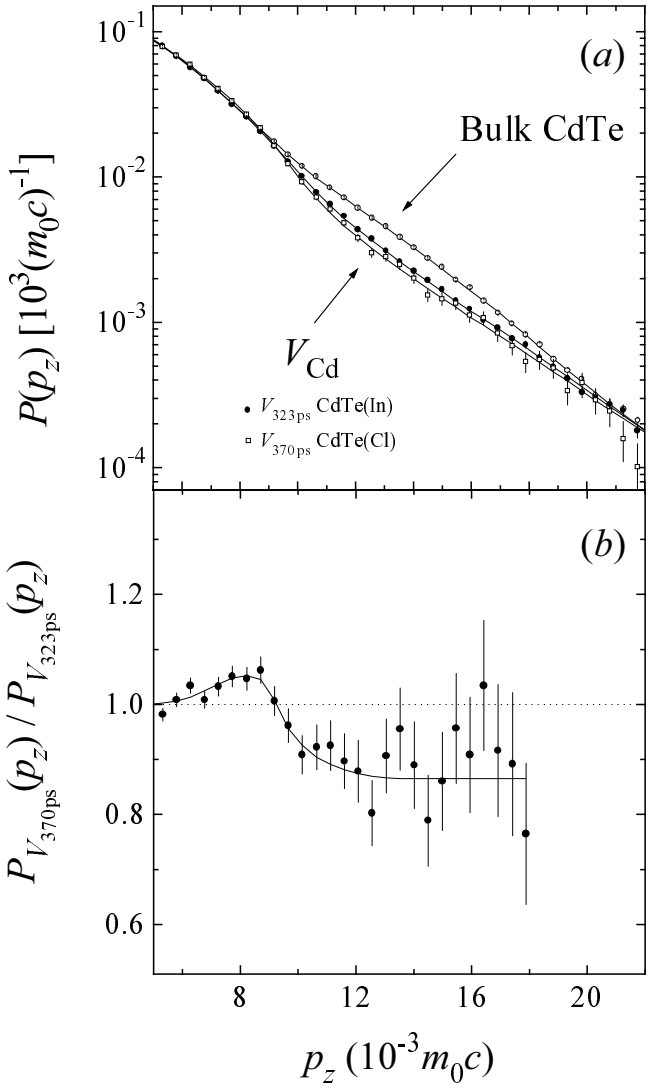

Figure 3. (*a*) High-momentum parts of the positron annihilation momentum densities $P(p_z)$ at the 323 ps vacancy in CdTe(In) (average of samples 3 and 4), at the 370 ps vacancy in CdTe(Cl) (average of samples 6 and 7) and in bulk CdTe (sample 1); (*b*) the ratio of the momentum density $P_{V_{370\,ps}}(p_z)$ at the 370 ps vacancy to the momentum density $P_{V_{323\,ps}}(p_z)$ at the 323 ps vacancy. The full curves are guides to the eye.

trapping fractions η_v are different. Second, both $P_b(p_z)$ as well as $P_v(p_z)$ change their slopes at 10–12 $\times$ $10^{-3}m_0c$ as indicated by the small arrows in figures 1 and 2. The low- and high-momentum parts of the distributions can be attributed to the valence and core-electron momentum distributions, respectively. Third, the high-momentum part of the vacancy response $P_v(p_z)$ in both $V_{323\,ps}$ and $V_{370\,ps}$ is lower than that of the bulk response $P_b(p_z)$. The difference between the vacancy and the bulk is confined to the momentum range (10–20) $\times$ $10^{-3}m_0c$, which is pointed out by the ratio plots $P_v(p_z)/P_b(p_z)$ in figures 1(*b*) and 2(*b*).

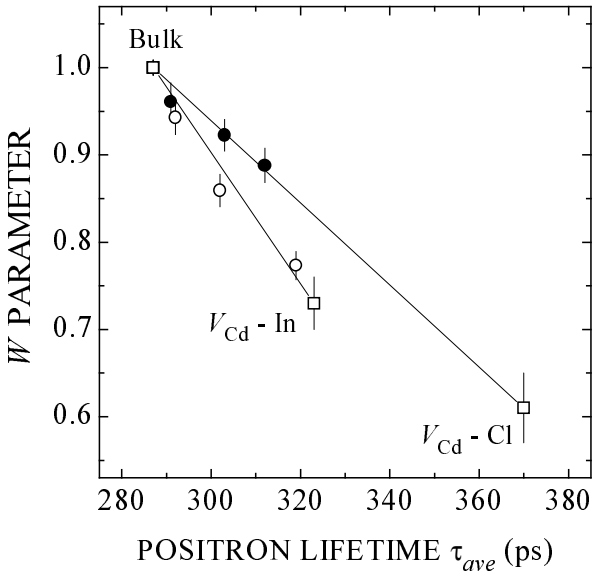

Figure 4. Determination of the characteristic W-parameters of the 323 ps vacancy in CdTe(In) and the 370 ps vacancy in CdTe(Cl). The open and full circles represent the data in the In- and Cl-doped CdTe-samples, respectively, the numerical values of the data are given in table 1.

3.2. Identification of cadmium vacancies

In CdTe(In) the $V_{323\,ps}$ vacancy is characterized by the positron lifetime ratio $\tau_v/\tau_b = 323/287 = 1.13$, which is indicative of a monovacancy defect. In CdTe(Cl) the $V_{370\,ps}$ vacancy is characterized by the positron lifetime ratio $\tau_v/\tau_b = 370/287 = 1.29$, which suggests that there is a substantial outwards lattice relaxation at the vacancy. The results are similar to those already reported [16–19].

Direct physical evidence of the identity of the $V_{323\,ps}$ and $V_{370\,ps}$ vacancies is obtained from the shapes of the positron annihilation momentum densities $P(p_z)$. We focus our interest on the high-momentum regions $p_z > 12 \times 10^{-3} m_0 c$ of $P_v(p_z)$ and $P_b(p_z)$ in figure 3. It is obvious that the distributions $P_v(p_z)$ at the vacancies $V_{323\,ps}$ and $V_{370\,ps}$ are more gently sloping than the bulk distribution $P_b(p_z)$ in the CdTe lattice. In other words, the distributions $P_v(p_z)$ have a broader shape than the distribution $P_b(p_z)$.

The shape difference can be understood on the basis of calculations of positron annihilation momentum densities $P(p_z)$ in bulk compound semiconductors. The following simple arguments are obtained from the results shown for GaAs, GaSb and InP in our earlier works [1, 2]: (i) the high-momentum part of $P(p_z)$ results dominantly from positron annihilations with the outermost d-electrons; (ii) in the bulk lattice the high-momentum part of $P_b(p_z)$ results dominantly from annihilations with the cation core electrons; and (iii) the momentum distributions of the anion core electrons are broader (i.e. more delocalized in momentum space) than the momentum distributions of the cation core electrons, because the anion core-electron orbitals are more localized in the direct space.

The theoretical arguments can now be used to interpret figure 3. The high-momentum part of $P_b(p_z)$ in bulk CdTe is expected to result dominantly from annihilations with Cd 4d electrons. The broader shape of $P_v(p_z)$ must be due to annihilations with more localized anion electrons, that is, with Te 4d electrons. The vacancy should then be in the cadmium sublattice, where the nearest-neighbour atoms of the vacancy are tellurium atoms.

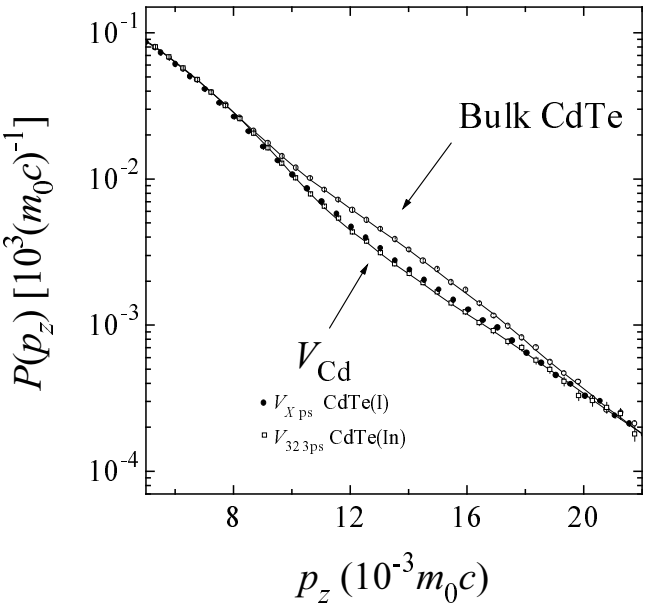

Figure 5. High-momentum parts of the positron annihilation momentum densities $P(p_z)$ at a vacancy defect in CdTe(I) (sample 11), at the 323 ps vacancy in CdTe(In) (average of samples 3 and 4) and in bulk CdTe (sample 1). The full curves are guides to the eye.

In conclusion, both $V_{323\,ps}$ in CdTe(In) as well as $V_{370\,ps}$ in CdTe(Cl) contain a cadmium vacancy V_{Cd}.

Are the observed cadmium vacancies in CdTe(In) or CdTe(Cl) complexed with impurity atoms? In CdTe(In) the indium impurity is situated in the Cd sublattice and it can belong only to the second nearest neighbours of the cadmium vacancy. The indium atom ($Z = 49$) differs very little from the cadmium host atoms ($Z = 48$). Therefore the effect of a single In atom among the second nearest neighbours on the core-electron momentum distribution can be expected to be very small. As the vacancy concentration in CdTe(In) increases with increasing In concentration, it is logical to assume that the $V_{323\,ps}$ defect is a vacancy-impurity complex V_{Cd}-In [16]. The Doppler-broadening measurements do not give direct evidence of impurity decoration, but rather the signal $P_v(p_z)$ of V_{Cd}-In is close to that of an isolated cadmium vacancy V_{Cd}.

The cadmium vacancy concentration in CdTe(Cl) also increases with increasing doping concentration. The high positron lifetime $\tau_v = 370$ ps suggests that there is a strong outwards relaxation of the vacancy, which could be caused by the replacement of one of the first neighbour atoms by a chlorine impurity. Further evidence of the decoration can be found in the W–τ plot in figure 4. From equations (2) and (3) it follows that in the presence of one positron trap $W(\tau)$ is a linear function. The W-data has been extrapolated to obtain the defect specific values $W_v = 0.73(3)$ for $V_{323\,ps}$ and $W_v = 0.61(4)$ for $V_{370\,ps}$. In a similar way from S-data of table 1 we can extract the defect specific S-values $S_v = 1.016(3)$ for $V_{323\,ps}$ and $S_v = 1.019(4)$ for $V_{370\,ps}$. From figure 4 it is evident that $\Delta W/\Delta\tau$ for $V_{323\,ps}$ is different than that for $V_{370\,ps}$. Such a result is not expected to be caused only by a difference in the lattice relaxations at the vacancies, but it implies rather that the neighbourhood of $V_{370\,ps}$ is chemically different due to the presence of the Cl impurity.

We assign the $V_{370\,ps}$ defect to the V_{Cd}-Cl complex. The effect of the Cl atom on the $P_v(p_z)$ distribution can be explained by its 3s and 3p valence electrons. These electrons are relatively tightly bound and produce a contribution to the high-momentum part. Therefore despite the large differences in the open volumes (positron lifetimes) the $P_v(p_z)$ distributions are rather alike for V_{Cd}-In and V_{Cd}-Cl. Above $p_z = 10 \times 10^{-3} m_0 c$ $P_{V_{Cd}-Cl}(p_z)$ is lower but between $p_z = (6\text{–}9) \times 10^{-3} m_0 c$ it is higher than $P_{V_{Cd}-In}(p_z)$ as can be seen from the ratio curve in figure 3(b).

We conclude that the Doppler-broadening measurements give direct evidence that the $V_{323\,ps}$ defect in CdTe(In) as well as the $V_{370\,ps}$ defect in CdTe(Cl) contain a cadmium vacancy V_{Cd}. The $V_{323\,ps}$ defect is likely to be a V_{Cd}-In complex, but the experimental method is insensitive to the In impurities. In CdTe(Cl) the Doppler-broadening results support the identification of the $V_{370\,ps}$ defect as the V_{Cd}-Cl complex and the effect of the Cl impurity is also visible in the momentum distribution $P_v(p_z)$.

4. Vacancy defects in MBE-grown CdTe(I) layers

The results obtained above are now applied to identify lattice defects in the MBE-grown CdTe(I) overlayers, in the case where positron lifetime data is not available. The S-parameters measured in the layers are given in table 2. We notice that the S-parameter increases as the I-dopant concentration increases to 2×10^{19} cm^{-3} and seems to saturate to a value $S = 1.018(1)$ when [I] $\geqslant 2 \times 10^{19}$ cm^{-3}. The saturation of S is accompanied by the onset of the free-carrier compensation [20].

The saturation of the S-parameter can be taken as an indication of saturation of positron trapping to a vacancy defect, when [I] $\geqslant 2 \times 10^{19}$ cm^{-3}. The electron momentum distribution $P(p_z)$ measured in sample 11 is then the distribution $P_v(p_z)$ characteristic to the vacancy. The electron momentum distribution $P(p_z)$ in the undoped sample 8 is identical to the bulk distribution $P_b(p_z)$ obtained in section 3.

Figure 5 shows that the high-momentum part of $P_v(p_z)$ at the vacancy in CdTe(I) is very similar to $P_v(p_z)$ at the V_{Cd}-In measured in CdTe(In). On the basis of the same arguments as in section 3, we can say that the broader shape of $P_v(p_z)$ in comparison with $P_b(p_z)$ results from annihilations with Te 4d electrons. The vacancy defect in CdTe(I) is then in the cadmium sublattice. The characteristic W-parameter of this vacancy is $W_v = 0.78(1)$.

The increasing of the vacancy concentration with increasing impurity concentration suggests that the cadmium vacancy in CdTe(I) is paired with an iodine atom. The I-atom ($Z = 53$) differs very little from the tellurium host atoms ($Z = 52$). Therefore, as in the case of CdTe(In), it is also believed here that the I impurity is not likely to be distinguished experimentally in the electron momentum distribution, although it may be a first neighbour of V_{Cd}. The characteristic W-parameter of the vacancy $W_v = 0.78(1)$ is also close to the value $W_v = 0.73(3)$ obtained for V_{Cd}-In, which indicates that the lattice relaxations and the open volumes at the two defects are quite similar.

In conclusion, the comparison of the $P_v(p_z)$ distribution at the vacancy defect in MBE-grown CdTe(I) with that of a V_{Cd}-In in CdTe(In) shows that the defect in MBE-grown CdTe(I) contains a cadmium vacancy V_{Cd}. We suggest that the vacancy is the V_{Cd}-I pair.

5. Conclusions

The high-momentum part of the positron annihilation momentum density $P(p_z)$ was measured in variously doped CdTe materials in order to determine the chemical identity of the defects. In CdTe(In) and CdTe(Cl) crystals, the defect specific momentum density at

vacancies $P_v(p_z)$ was determined by combining positron lifetime and Doppler-broadening measurements. In MBE-grown CdTe(I) overlayers, $P_v(p_z)$ was obtained by Doppler-broadening measurements with a low-energy positron beam. The high-momentum part of $P(p_z)$ was resolved with a two-detector system where the background is reduced by detecting the both annihilation photons in coincidence.

In CdTe(In) and CdTe(Cl), positron lifetime measurements show vacancy defects with characteristic positron lifetimes of 323 ps and 370 ps, respectively. In MBE-grown CdTe(I), positron trapping to vacancies is observed by Doppler-broadening experiments. The high-momentum part of $P_v(p_z)$ at vacancies in In-, Cl- and I-doped CdTe is broader than that of the distribution $P_b(p_z)$ in the CdTe bulk lattice. This indicates that positrons annihilate with the more localized Te 4d core electrons when trapped at vacancies, whereas in bulk CdTe the core-electron annihilation occurs mostly with the less localized Cd 4d core electrons. The Doppler-broadening results show that $V_{323\,ps}$ in CdTe(In), $V_{370\,ps}$ in CdTe(Cl) as well as the vacancy in CdTe(I) contain a cadmium vacancy V_{Cd}.

The cadmium vacancy concentrations increase with the donor-impurity contents suggesting that the defects are vacancy–donor complexes. As the In- and I-impurities are very similar to the host atoms Cd and Te, respectively, the impurity decoration in V_{Cd}-In and V_{Cd}-I is not clearly observed in the Doppler-broadening experiments. In CdTe(Cl), it seems that the Cl-impurity contributes to the $P_v(p_z)$ distribution and thus evidence is found that the defect is a vacancy–impurity complex V_{Cd}-Cl.

References

[1] Alatalo M, Kauppinen H, Saarinen K, Puska M J, Mäkinen J, Hautojärvi P and Nieminen R M 1995 *Phys. Rev.* B **51** 4176

[2] Alatalo M, Barbillieni B, Hakala M, Kauppinen H, Korhonen T, Puska M J, Saarinen K, Hautojärvi P and Nieminen R M 1996 *Phys. Rev.* B **54** 2397

[3] Laine T, Mäkinen J, Saarinen K, Hautojärvi P, Corbel C, Fille M L and Gibart G 1996 *Phys. Rev.* B **53** 11 025

[4] Mäkinen J *et al* 1996 *Phys. Rev.* B **53** 7851

[5] Saarinen K, Laine T, Skog K, Mäkinen J, Hautojärvi P, Rakennus K, Uusimaa P, Salokatve A and Pessa M 1996 *Phys. Rev. Lett.* **77** 3407

[6] Szpala S, Asoka-Kumar P, Nielsen B, Peng J P, Hayakawa S, Lynn K G and Gossmann H-J 1996 *Phys. Rev.* B **54** 4722

[7] Asoka-Kumar P, Alatalo M, Ghosh V J, Kruseman A C, Nielsen B and Lynn K G 1996 *Phys. Rev. Lett.* **77** 2097

[8] Hautojärvi P and Corbel C 1995 *Positron Spectroscopy of Solids* ed A Dupasquier and A P Mills Jr (Amsterdam: IOS) p 491
Corbel C and Hautojärvi P 1995 *Positron Spectroscopy of Solids* ed A Dupasquier and A P Mills Jr (Amsterdam: IOS) p 533

[9] Puska M J and Nieminen R M 1994 *Rev. Mod. Phys.* **66** 641

[10] Lynn K G and Goland A N 1976 *Solid State Commun.* **18** 1549

[11] Hage-Ali M and Siffert P 1992 *Nucl. Instrum. Methods* A **322** 313

[12] Emmanuelsson P, Omling P, Meyer B K, Wienecke M and Schenck M 1993 *Phys. Rev.* B **47** 15 578

[13] Hoffmann D M, Omling P, Grimmeiss H G, Meyer B K, Benz K W and Sinerius D 1992 *Phys. Rev.* B **45** 6247

[14] Meyer B K, Omling P, Weigel E and Müller-Vogt G 1992 *Phys. Rev.* B **46** 15 135

[15] Plazaola F, Seitsonen A P and Puska M J 1994 *J. Phys.: Condens. Matter* **6** 8809

[16] Gély-Sykes C, Corbel C and Triboulet R 1991 *Solid State Commun.* **80** 79

[17] Gély C, Corbel C and Triboulet R 1989 *C. R. Acad. Sci., Paris* **309** 179

[18] Polity A, Abgarjan Th and Krause-Rehberg R 1995 *Mater. Sci. Forum* **175–178** 473

[19] Baroux L, Liszkay L and Corbel C, to be published

[20] Fischer F, Waag A, Worschech L, Ossau W, Scholl S, Landwehr G, Mäkinen J, Hautojärvi P and Corbel C 1996 *J. Crystal Growth* **161** 214